

Supplementary Information

Photochemical vapor generation of platinum in mixed formic acid and acetic acid: Enhanced effect from cobalt and molybdate ions

Ying Yu^{†,§}, Kezhu Yuan^{†,§}, Liang Dong[†], Ying Gao^{†*}

[†] State Key Laboratory of Geohazard Prevention and Geoenvironment Protection, College of Earth Sciences, Chengdu University of Technology, Sichuan 610059, China

[§] Ying Yu and Kezhu Yuan made equal contributions to this work.

Corresponding author E-mail: Ying.gaoy@gmail.com;

Table of Contents

Fig. S1. Effect of LMWOAs concentration and UV irradiation time on the detection of Pt-----	S3
Fig. S2. Comparison of signal responses of Pt in different LMWOAs medium-----	S4
Fig. S3. The effect of UV irradiation time on Pt responses equipped with germicidal lamp-----	S5
Fig. S4. Effect of Ar carrier gas flow rate on Pt detection-----	S6
Fig. S5. Comparison of signal responses of Pt in different PVG system-----	S7
Fig. S6. The effect of UV irradiation time on Pt responses equipped with germicidal lamp-----	S8
Fig. S7. Comparison of signal responses of Pt in different PVG reactor-----	S9
Fig. S8. Comparison of signal responses of Pt in different PVG media-----	S10
Fig. S9. UV-vis absorbance of different medium before and after PVG reaction-----	S11
Fig. S10. The high-resolution XPS spectra of Pt 4f and Mo 3d of liquid products after PVG-----	S12
Fig. S11. Time-resolved profiles and the signal responses of Mo-----	S13
Fig. S12. Schematic diagram of the PVG system operating in dual-carrier-gas configuration-----	S14
Fig. S13. Comparison of signal responses of 2 μ g L ⁻¹ Pt in different carrier-gas mode-----	S15
Fig. S14. The high-resolution XPS spectra of Pt 4f and Co 2p of liquid products after PVG-----	S16
Fig. S15. Comparison of analytical sensitivity of different PVG systems for Pt detection with dual-carrier-gas mode-----	S17
Fig. S16. Comparison of PVG efficiency in different PVG system-----	S18
Fig. S17. Effect of FA and AA concentration on the detection of Pd/Rh/Ru-----	S19
Table S1. ICP-MS instrumental operating conditions-----	S20
Table S2. Impacts of co-existing ions/ acids on detection of Pt-----	S21
Text S1. Instrumentation-----	S23
Text S2. Reagents and Materials-----	S24
Text S3. GC MS, TEM-EDS and XPS Characterization-----	S25
Reference-----	S26

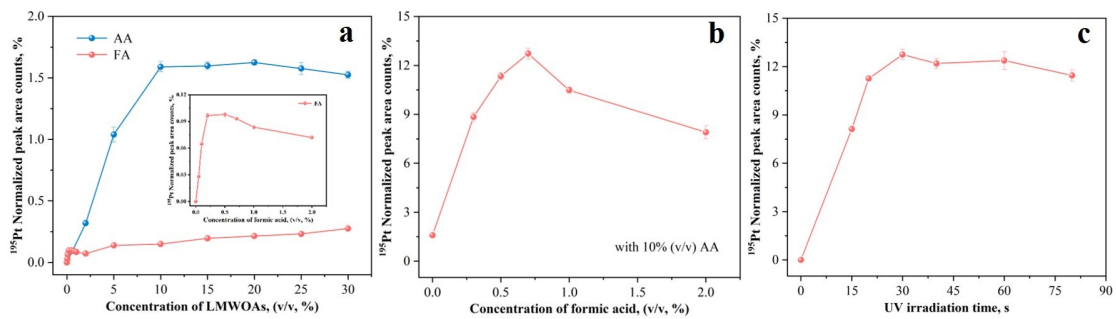


Fig. S1. Effect of concentration of LMWOAs (a), FA (b) and UV irradiation time (c) on the detection of $2.0 \mu\text{g L}^{-1}$ Pt: 10% (v/v) AA, 0.7% (v/v) FA, or 30 s UV irradiation.

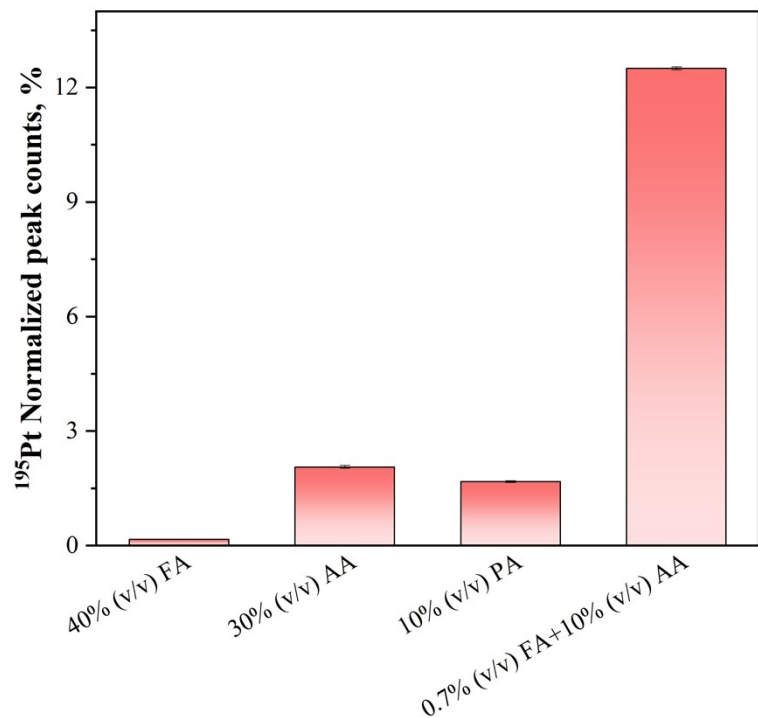


Fig. S2. Comparison of signal responses of $2 \mu\text{g L}^{-1}$ Pt in different LMWOAs medium: 40% (v/v) FA with 20 s for UV irradiation; 30% (v/v) AA with 60 s for UV irradiation; 10% (v/v) PA with 90 s for UV irradiation; 0.7% (v/v) FA and 10% (v/v) AA with 30 s for UV irradiation.

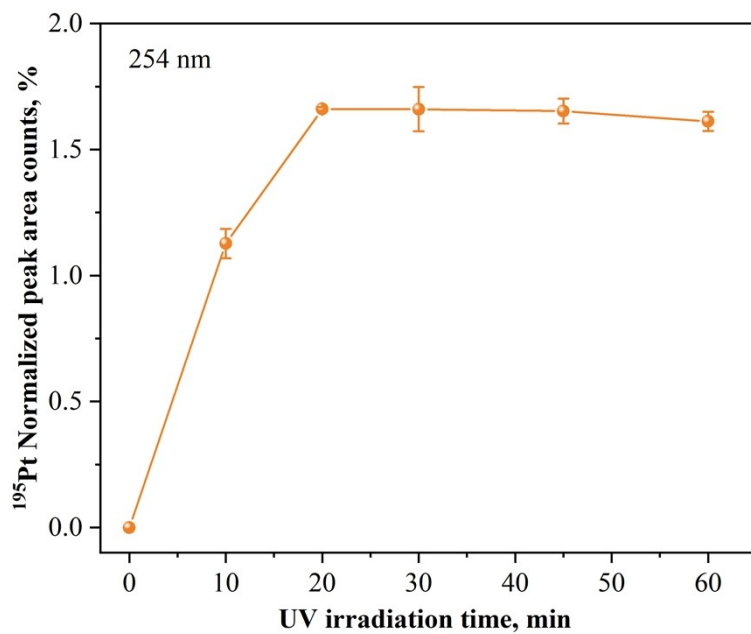


Fig. S3. The effect of UV irradiation time on $2.0 \mu\text{g L}^{-1}$ of Pt responses equipped with germicidal lamp: 5% (v/v) AA, 1% (v/v) FA and 10.0 mg L^{-1} Mo(VI).

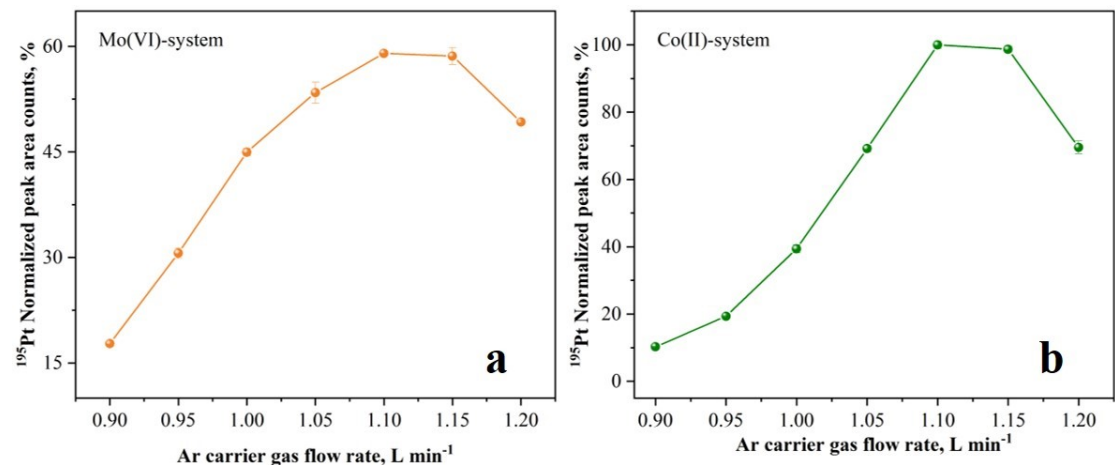


Fig. S4. Effect of Ar carrier gas flow rate on 2.0 $\mu\text{g L}^{-1}$ Pt detection. (a) Mo(VI)-system: 5% (v/v) AA, 1% (v/v) FA, 10.0 mg L^{-1} Mo(VI), and 50 s UV irradiation time; (b) Co(II)-system: 5% (v/v) AA, 0.2% (v/v) FA, 20.0 mg L^{-1} Co(II), and 25 s UV irradiation time.

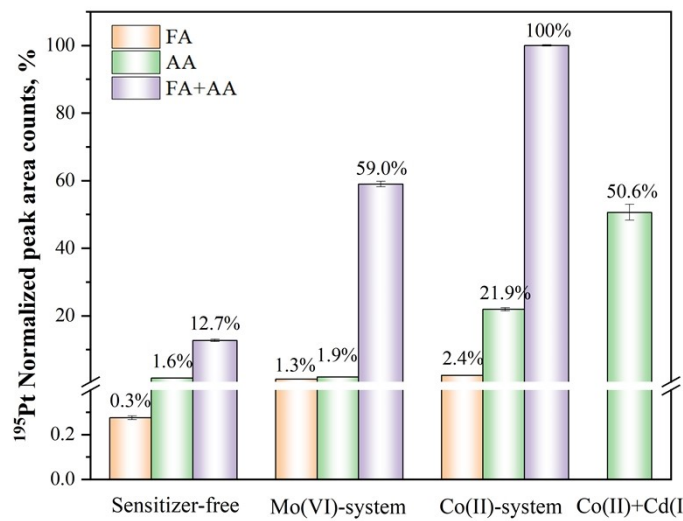


Fig. S5. Comparison of signal responses of Pt in different PVG system. Sensitizer-free system: 30% (v/v) FA, 10% (v/v) AA, or 0.7% (v/v)FA+10% (v/v)AA, with 30 s UV irradiation time; Mo(VI)-system: 0.2% (v/v) FA, 5% (v/v) AA, or 1% (v/v)FA+10% (v/v)AA, with 10.0 mg L⁻¹ Mo(VI), and 50 s UV irradiation time; Co(II)-system: 0.007% (v/v) FA, 5% (v/v) AA, or 0.2% (v/v)FA+5% (v/v)AA, with 20.0 mg L⁻¹ Co(II), and 25 s UV irradiation time; Co(II)+Cd(II)-system: 30% (v/v) AA, 10.0 mg L⁻¹ Co(II), 5.0 mg L⁻¹ Cd(II), and 60 s UV irradiation time.

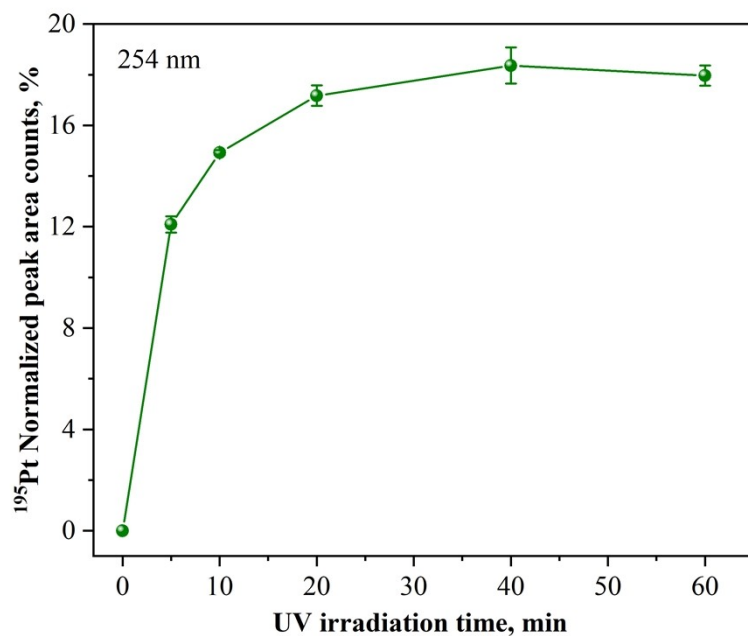


Fig. S6. The effect of UV irradiation time on $2.0 \mu\text{g L}^{-1}$ of Pt responses equipped with germicidal lamp: 5% (v/v) AA, 0.2% (v/v) FA and 20.0 mg L^{-1} Co(II).

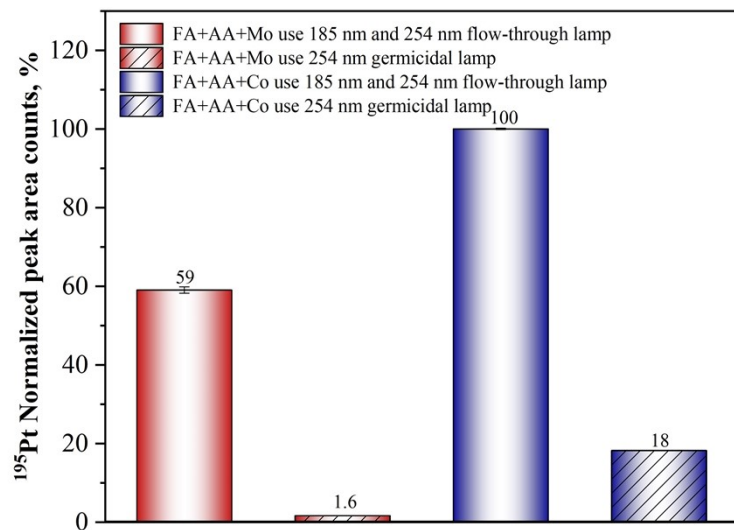


Fig. S7. Comparison of signal responses of $2 \mu\text{g L}^{-1}$ Pt in different PVG reactor. (a) Mo(VI)-system: 5% (v/v) AA, 1% (v/v) FA, 10.0 mg L^{-1} Mo(VI), and 50 s UV irradiation time. (b) Co(II)-system: 5% (v/v) AA, 0.2% (v/v) FA, 20.0 mg L^{-1} Co(II), and 25 s UV irradiation time.

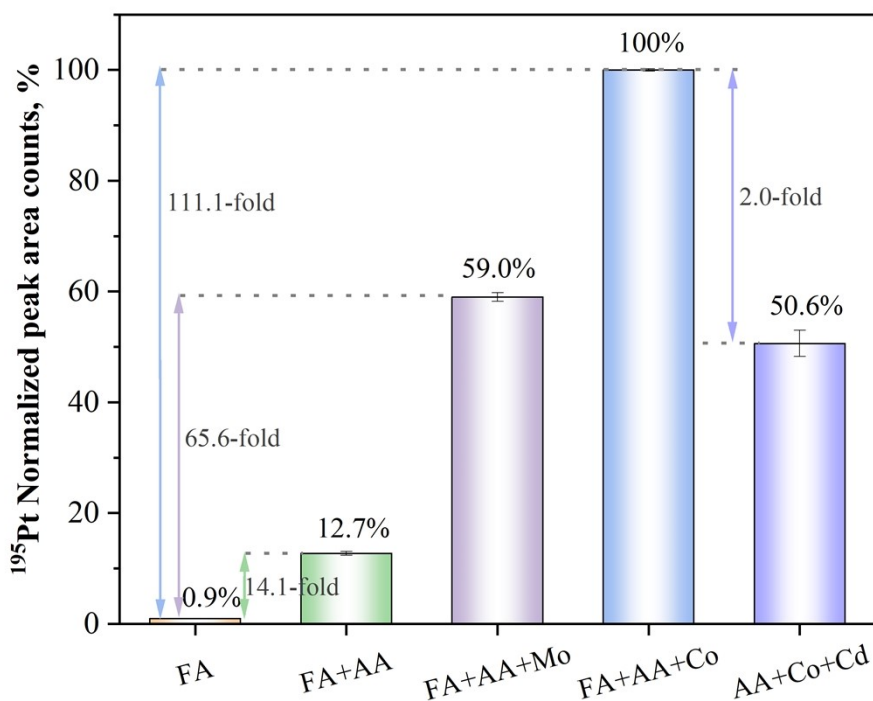


Fig. S8. Comparison of signal responses of $2 \mu\text{g L}^{-1}$ Pt in different PVG media. FA-system: 20% (v/v) FA, and 45 s UV irradiation time. FA+AA-system: 0.7% (v/v) FA, 10% (v/v) AA, and 30 s UV irradiation time; Mo(VI)-system: 5% (v/v) AA, 1% (v/v) FA, 10.0 mg L^{-1} Mo(VI), and 50 s UV irradiation time; Co(II)-system: 5% (v/v) AA, 0.2% (v/v) FA, 20.0 mg L^{-1} Co(II), and 25 s UV irradiation time; Co(II)+Cd(II)-system: 30% (v/v) AA, 10.0 mg L^{-1} Co(II), 5.0 mg L^{-1} Cd(II), and 60 s UV irradiation time.

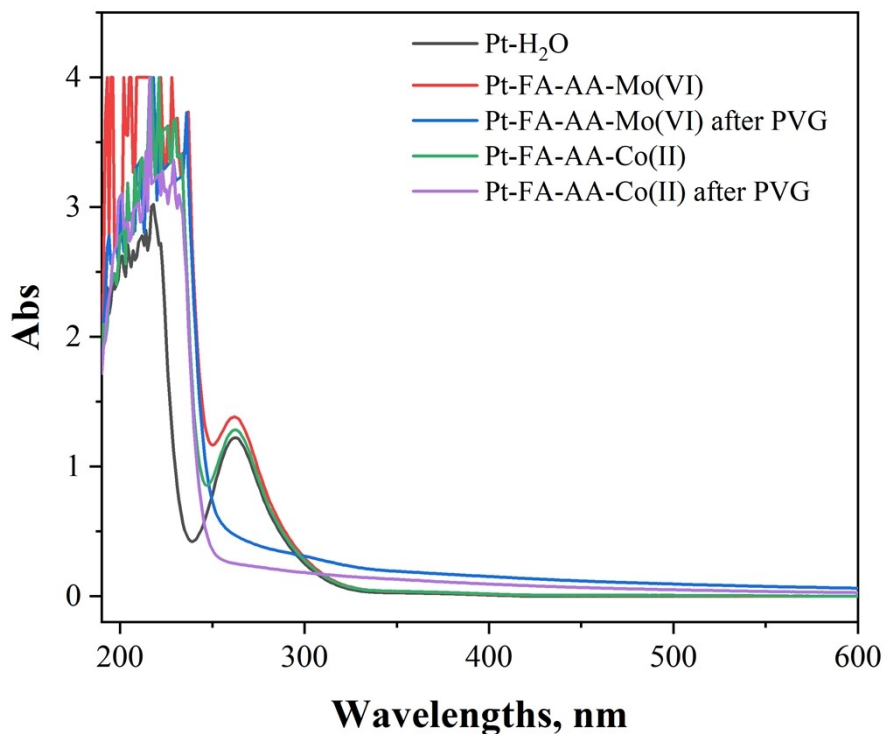


Fig. S9. UV-vis absorbance of different medium before and after PVG reaction: 1% (v/v) FA, 5% (v/v) AA, 10 mg L⁻¹ Mo(VI) for Mo(VI)-assisted system; 0.2% (v/v) FA, 5% (v/v) AA, 20 mg L⁻¹ Co(II) for Co(II)-assisted system; the concentration of Pt was kept at 10 mg L⁻¹ in UV-Vis.

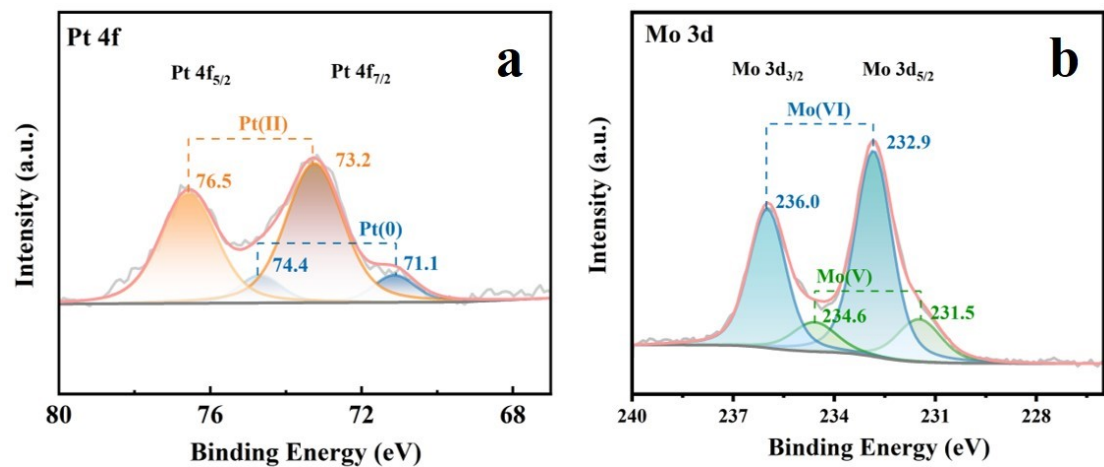


Fig. S10. The high-resolution XPS spectra of Pt 4f (a) and Mo 3d (b) of liquid products after PVG. 20 mg L⁻¹ Pt, 5% (v/v) AA, 1% (v/v) FA, 10.0 mg L⁻¹ Mo(VI), and 50 s UV irradiation time.

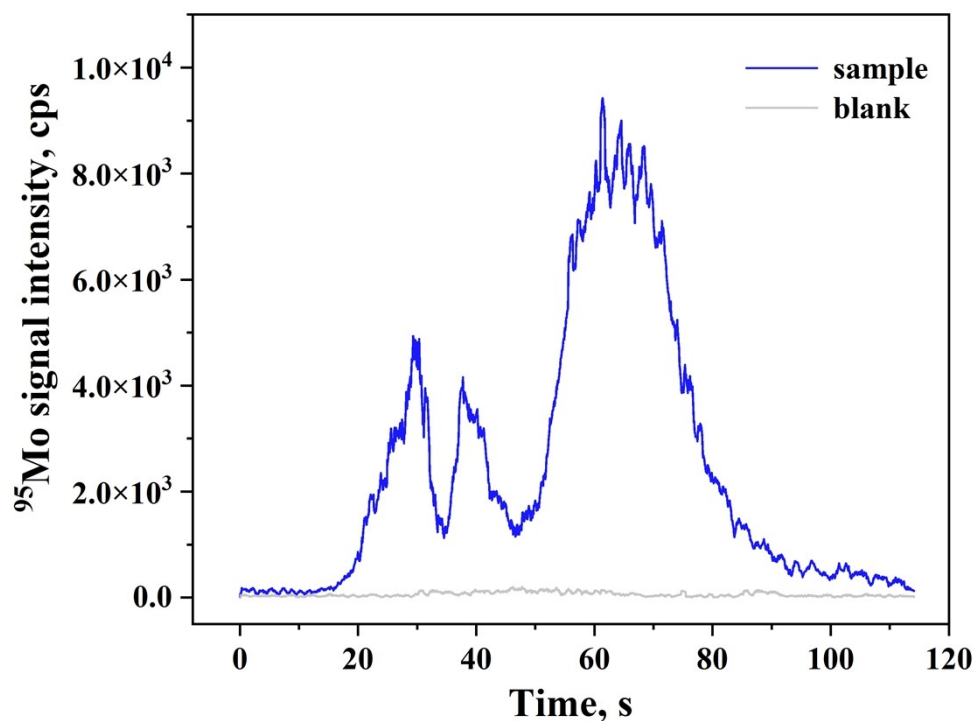


Fig. S11. Time-resolved profiles and the signal responses of Mo. 1% (v/v) FA, 5% (v/v) AA, 10 mg L⁻¹ Mo(VI), 50 s UV irradiation.

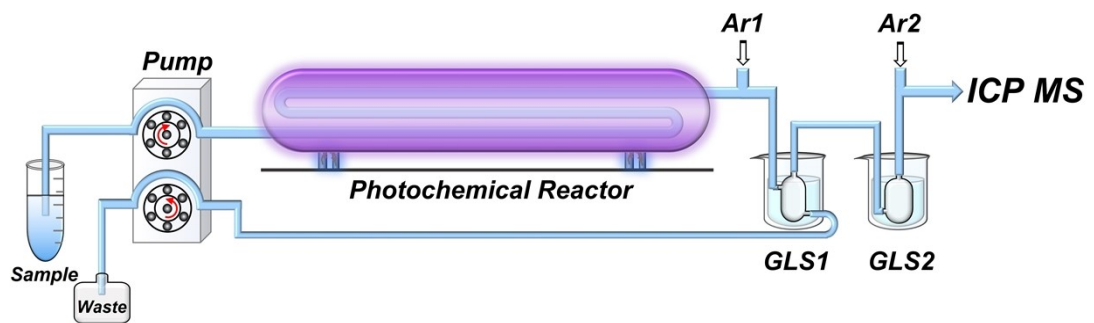


Fig. S12. Schematic diagram of the PVG system operating in dual-carrier-gas configuration.

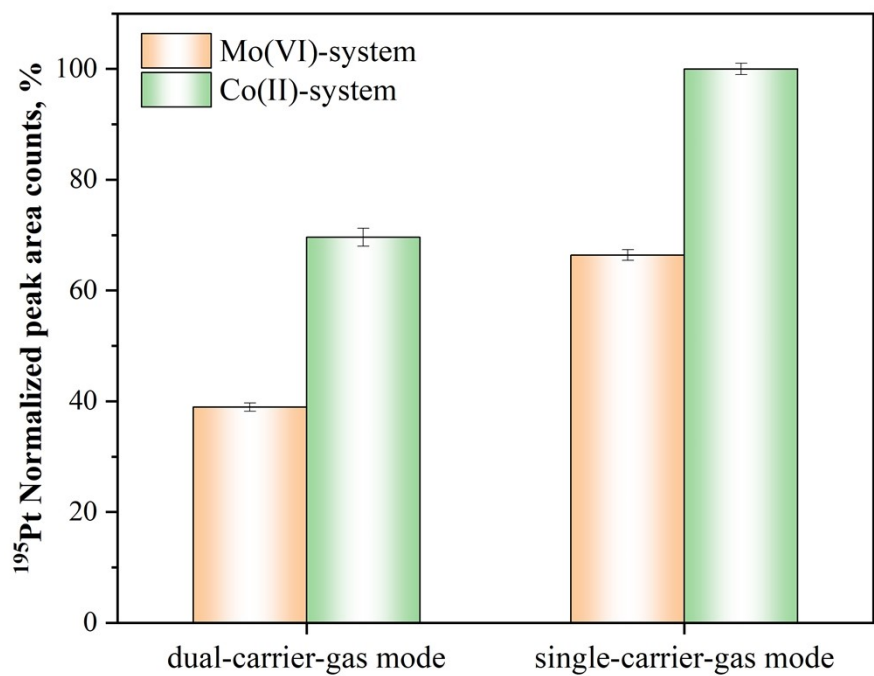


Fig. S13. Comparison of signal responses of $2 \mu\text{g L}^{-1}$ Pt in different carrier-gas mode. Dual-carrier-gas mode: 0.1 L min^{-1} Ar1 carrier gas flow rate and 1.0 L min^{-1} Ar2 carrier gas flow rate; single-carrier-gas mode: 1.1 L min^{-1} Ar carrier gas flow rate.

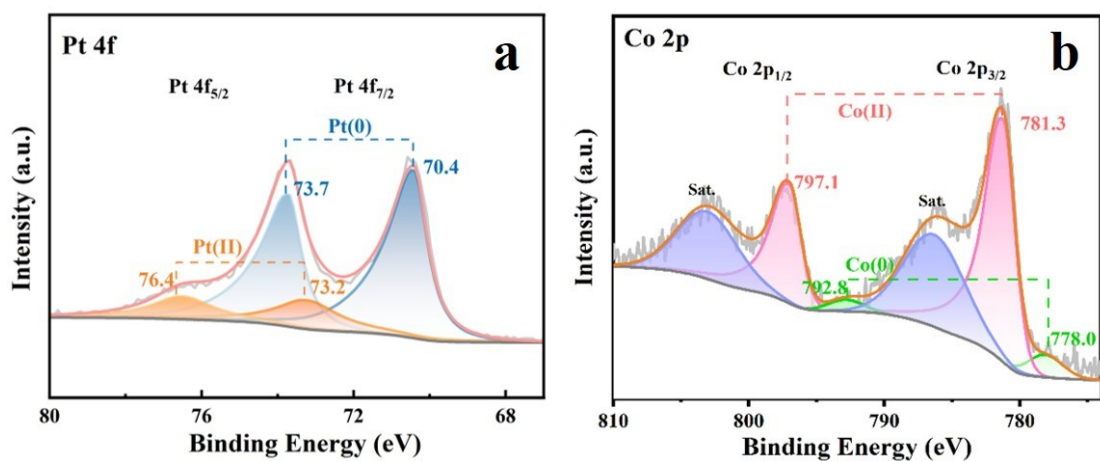
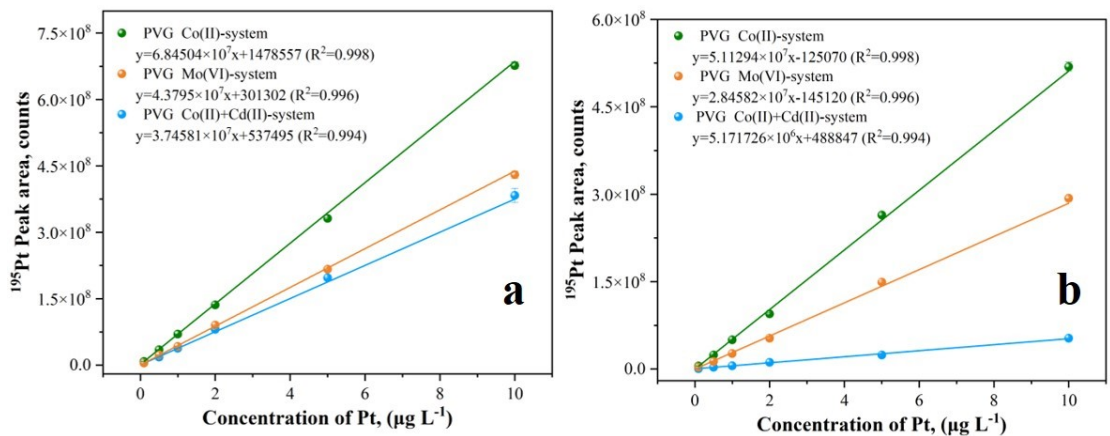


Fig. S14. The high-resolution XPS spectra of Pt 4f (a) and Co 2p (b) of liquid products after PVG. 20 mg L⁻¹ Pt, 5% (v/v) AA, 0.2% (v/v) FA, 20.0 mg L⁻¹ Co(II), and 25 s UV irradiation time.



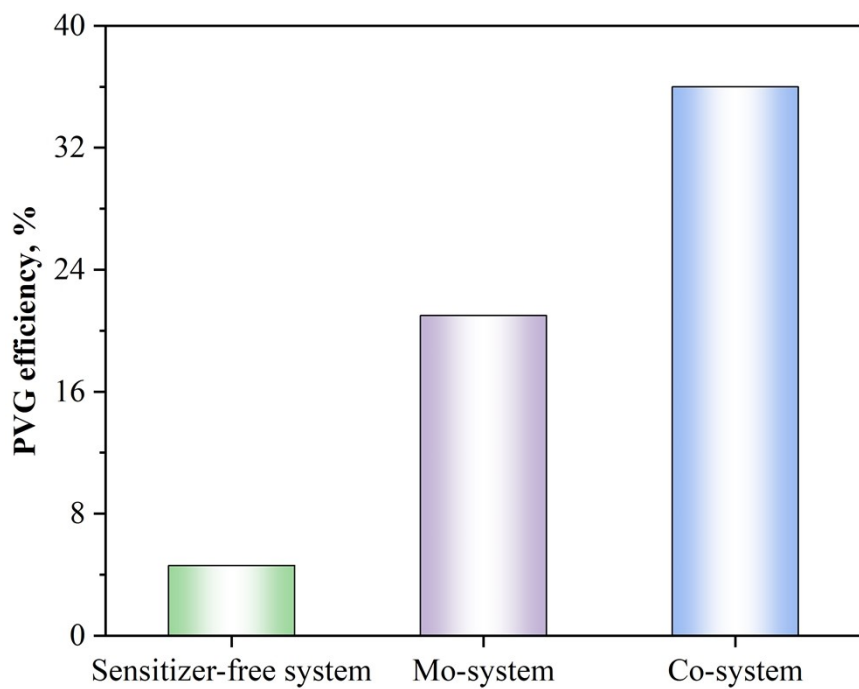


Fig. S16. Comparison of PVG efficiency in different PVG system. Sensitizer-free system: 0.7% (v/v)FA, 10% (v/v)AA, and 30 s UV irradiation time; Mo(VI)-system: 5% (v/v) AA, 1% (v/v) FA, 10.0 mg L⁻¹ Mo(VI), and 50 s UV irradiation time. Co(II)-system: 5% (v/v) AA, 0.2% (v/v) FA, 20.0 mg L⁻¹ Co(II), and 25 s UV irradiation time.

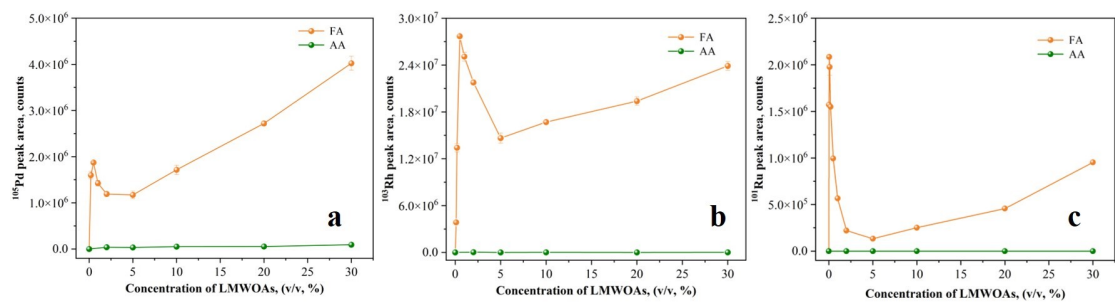


Fig. S17. Effect of FA and AA concentration on the detection of Pd/Rh/Ru: 10.0 ng mL⁻¹ Pd/Rh or 50 ng mL⁻¹ Ru and 30 s UV irradiation time.

Table S1. ICP MS instrumental operating conditions.

Instrument settings	Value
Sample flow rate	4.8 mL min ⁻¹
Auxiliary Ar gas flow rate	1.2 L min ⁻¹
Plasma Ar gas flow rate	15 L min ⁻¹
Ar carrier gas flow rate	1.1 L min ⁻¹
RF power	1150 W
Dwell time	50 ms
Dead time	35 ns
Scanning mode	Peak hopping
Isotopes monitored	¹⁹⁵ Pt

Table S2. Impacts of co-existing ions/ acids on detection of 2.0 $\mu\text{g L}^{-1}$ Pt.

Interfering ions	Used reagents	Mo(VI)-system		Co(II)-system	
		Concentration (mg L ⁻¹)	Recovery% (n=3)	Concentration (mg L ⁻¹)	Recovery% (n=3)
Na ⁺	Na ₂ SO ₄	50	100±1	50	103±1
Mg ²⁺	Mg ₂ SO ₄	50	98±3	50	101±3
K ⁺	K ₂ SO ₄	50	99±2	50	100±2
Ca ²⁺	CaCl ₂	50	101±1	50	99±3
V ⁵⁺	NH ₄ VO ₃	10	85±3	20	105±1
Cr ³⁺	Cr ₂ (SO) ₄	20	104±2	20	103±3
Zn ²⁺	ZnSO ₄ ·7H ₂ O	20	102±2	20	94±2
Cd ²⁺	CdCl ₂	5	103±1	10	106±1
Cu ²⁺	CuSO ₄	10	96±1	20	99±2
Pb ²⁺	PbCl ₂	10	101±1	1	106±2
Se ⁴⁺	Na ₂ SeO ₃	0.005	91±15	0.005	86±1
Se ⁶⁺	Na ₂ SeO ₄	0.01	85±1	0.05	95±1
Te ⁴⁺	Na ₂ TeO ₃	0.2	86±2	0.2	87±2
Te ⁶⁺	Na ₂ TeO ₅ ·2H ₂ O	0.5	88±1	1	82±1
Bi ³⁺	Standard solution	0.2, 0.5	94±1, 84±2	5	94±2
Cl ⁻	NaCl	50	91±3	50	92±4
SO ₄ ²⁻	Na ₂ SO ₄	50	98±2	50	97±1
NO ₃ ⁻	NaNO ₃	5, 10	96±2, 84±2	20	94±3
HCl	HCl	0.01%, 0.02%	95±4, 62±3	0.02%, 0.05%	92±2, 83±4
H ₂ SO ₄	H ₂ SO ₄	0.2%, 0.5%	99±1, 68±2	0.5%, 1%	94±1, 64±2
HNO ₃	HNO ₃	0.0005%, 0.001%	95±2, 72±3	0.05%, 0.01%	93±2, 86±3

In both systems, 50 mg L⁻¹ of Na(I), Mg(II), K(I) and Ca(II), as well as 20 mg L⁻¹ of Cr(III) and Zn(II), had no significant effect on the determination of 2 ng mg L⁻¹ Pt. For the Co(II) system, 20 mg mg L⁻¹ V(V) and 10 mg L⁻¹ Cd(II) were also tolerated, whereas the Mo(VI) system tolerated only 5 mg L⁻¹ of these ions.

A recently reported Co(II)-Cd(II) synergistic PVG system in FA or AA medium showed poor tolerance toward Cu(II) and Pb(II), resisting only a 20-fold excess of either ion.¹ In contrast, the mixed-acid medium proposed here raised the tolerance level to 10000-fold for Cu(II) and 5000-fold for Pb(II) in the Co(II)-assisted system, and to 5000-fold for Cu(II) and 500-fold for Pb(II) in the Mo(VI)-assisted system. Moreover,

no significant signal change was observed for 0.005 mg L^{-1} Se(IV) or 0.2 mg L^{-1} Te(IV). In the Co(II) system, 5 mg L^{-1} Bi(III), 0.05 mg L^{-1} Se(VI) and 1.0 mg L^{-1} Te(VI) were tolerated, whereas in the Mo(VI) system the corresponding maximum allowable concentrations dropped to 0.5 , 0.01 and 0.5 mg L^{-1} , respectively.

The influence of common anions and inorganic acids on the determination was also evaluated. In both PVG systems, 50.0 mg L^{-1} Cl^- and SO_4^{2-} did not noticeably affect Pt detection. Addition of 20.0 mg L^{-1} NO_3^- was tolerated in the Co(II) system, whereas 10 mg L^{-1} NO_3^- was tolerated in the Mo(VI) system without significant signal change. At 0.02% (v/v) HCl, no appreciable interference was observed for the Co(II) system, whereas the Pt signal in the Mo(VI) system dropped to 62% . Both systems were more tolerant to H_2SO_4 : 0.5% (v/v) H_2SO_4 left the Co(II) signal unchanged, while the Mo(VI) signal decreased to 68% . HNO_3 strongly suppressed analyte reduction and volatile-species formation.² Addition of only 0.01% (v/v) HNO_3 to the Co(II) system decreased the Pt signal to 86% , and 0.001% (v/v) HNO_3 in the Mo(VI) system reduced it to 72% . Consequently, mineral acids should be avoided during sample acidification, or removed prior to analysis.

Text S1. Instrumentation

In this study, an ICP MS (LAB MS3000, Labtech Instruments Co., Ltd., Beijing, China) operating in time-resolved mode was utilized to determinate the signal responses of Pt, with PVG replacing the traditional pneumatic nebulizer, as shown in Figure 1. Sample solution was introduced by an IFIS-D type flow injection system (Xi'an Remex Analysis Instrument Co. Ltd., Xi'an, China). The PVG photoreactor consisted of a 19 W thin-film low-pressure mercury lamp (Beijing Titan Instruments Co., China) with an internal volume of approximately 1.0 mL, providing mainly 185 and 254 nm radiation. And the incident photon flux of flow-through UV lamp was found to be 18.86×10^{-6} E s⁻¹ using an iodide/iodate actinometer.³ To investigate the UV wavelengths on the photochemical reduction of Pt, a 15 W germicidal lamp (mainly emitting UV irradiation at 254 nm) was also employed as the photoreactor with 4.69×10^{-6} E s⁻¹ incident photon flux. Two gas liquid separators (GLSs, with an internal volume of about 5.0 mL) were used to separate the volatile substances generated during the photoreaction process and transfer them to ICP MS with Ar carrier gas assisted. The signal response of ¹⁹⁵Pt was detected, and quantification was based on the peak area, with the obtained values normalized to the highest signal in the Co(II)-assisted system. The main instrumental parameters for ICP-MS are listed in Table S1. A UV-Vis spectrophotometer (SP-756P, Shanghai Spectrum Instruments Co., Ltd., Shanghai, China) was used to detect the absorption spectra of different PVG media. The volatile substances were identified by gas chromatography-mass spectrometry instrument (GC-MS, Fuli-S900 GC-MSD, Zhejiang Fuli Analytical Instruments Co., Zhejiang, China). And the nanoparticles in the liquid-phase products after PVG reaction were characterized by transmission electron microscopy and energy dispersive spectroscopy (TEM-EDS, Tecnai G2 F20 STWIN 20, FEI Co., USA), and X-ray photoelectron spectroscopy (XPS, AXIS Ultra DLD 800x, Kratos Co., USA).

Text S2. Reagents and Materials

Deionized water (DIW) was used throughout the experiment. All reagents were of analytical grade or better. A 1000 mg L⁻¹ Pt standard solution was purchased from Aladdin Industrial Corporation (Shanghai, China) and diluted stepwise before use. A 1000 mg L⁻¹ As(III) and As(V) standard solution was purchased from WEIYE Metrology and Technology Research Group Co. (Beijing, China), and a 1000 mg L⁻¹ Bi(III) standard solution was purchased from the National Research Centre for Standard Materials (Beijing, China). Cobalt acetate, ferrous sulfate, copper sulfate, chromium sulfate, zinc sulfate, ammonium metavanadate, sodium selenite dihydrate, cadmium chloride, sodium tellurite, sodium selenate, sodium molybdate dihydrate, formic acid (FA, ACS grade), acetic acid (AA, ACS grade) were purchased from Aladdin Industrial Corporation (Shanghai, China). Sodium sulfate, magnesium sulfate, potassium sulfate, calcium chloride, nickel sulfate hexahydrate, sodium chloride, sodium nitrate, and sulfuric acid were purchased from KESHI Co. (Chengdu, China). Sodium selenate was purchased from XIYA Chemical Co., Ltd. (Chengdu, China). Three environmental water samples, including lake water, river water and tap water, collected near the campus of Chengdu University of Technology were pre-filtered with a 0.45 μ m filter and stored in 1% (v/v) AA.

Text S3. GC MS, TEM-EDS and XPS Characterization

For GC MS characterization, the volatile products were collected from the headspace of the first GLS of the PVG system using a gastight Hamilton syringe (5 mL). The operation parameters were set as follows: injector temperature at 150 °C, oven temperature program, 35 °C, hold for 10 min, heated to 150 °C at 30 °C min⁻¹; transfer line temperature at 150 °C. The carrier gas of He was at 1.2 mL min⁻¹.

For TEM-EDS and XPS characterization, the waste solutions were collected from the GLS of PVG system and directly dropped onto the copper mesh or silicon wafer. Then, the solutions were air-dried at room temperature, leaving the nanoparticles deposited on copper mesh or silicon wafer. To minimize oxidation by air, all sample preparation procedures were carried out in an argon-filled glove box.

Reference

1. X. Zou, Y. Zhang, H. Chen, J. Hu and X. Hou, *Anal. Chem.* 2025, **97**, 17931-17937.
2. R.E. Sturgeon, *J. Anal. At. Spectrom.* 2017, **32**, 2319-2340.
3. L.H. Kong, J.M. Zhao, X.Y. Hu, F. Zhu and X.J. Peng, *Environ. Sci. Technol.* 2022, **56**, 9732-9743.